Lechl *et al. Energy Informatics* 2023, **6**(Suppl 1):34
https://doi.org/10.1186/s42162-023-00273-4

Energy Informatics

RESEARCH Open Access

Aggregating multi-time-scale flexibility potentials of battery storages based on open data: a potential analysis

Michael Lechl[1*], Luis Schoppik[1] and Hermann de Meer[1]

From The 12th DACH+ Conference on Energy Informatics 2023
Vienna, Austria. 4-6 October 2023. https://www.energy-informatics2023.org/

*Correspondence:
michael.lechl@uni-passau.de

[1] University of Passau, Innstraße 41, 94032 Passau, Germany

Abstract

Flexibility potentials are mostly provided by centrally coordinated flexibility resources such as natural-gas-fired power plants. However, the decentralization of power generation combined with the decarbonization of the sector due to the energy transition requires the exploration of new types of flexibility resources. In particular, to reduce dependence on natural-gas-fired power plants, it would be desirable to replace them with alternative flexibility resources. Therefore, the objective of this paper is to analyze, using Germany as an example, to what extent the flexibility potential of already existing battery storage systems can replace the flexibility potential of natural-gas-fired power plants. The methodology used is based on a multi-time-scale flexibility model together with an approach for temporal aggregation of flexibility potentials and two approaches for spatial aggregation of flexibility potentials. Based on the methodology and an analysis of publicly available data, a comprehensive potential analysis is carried out. This analysis shows, among others, that existing battery storage systems have a promising potential to replace a considerable number of natural-gas-fired power plants in Germany in terms of their flexibility potentials.

Keywords: Flexibility modeling, Flexibility resources, Energy transition, Data analysis

Introduction

Flexibility is an important factor for a stable, economic, and sustainable operation of an electrical energy system. In literature, flexibility is commonly defined as the capability of an energy system to balance disturbances (e.g., intermittent Photovoltaic (PV) power generation) sufficiently fast to maintain stability (Lannoye et al. 2012; Bucher et al. 2015b; Huo et al. 2020). Such disturbances are referred to as *flexibility requirements* in the following. To balance flexibility requirements, energy systems use the *flexibility potential* of *flexibility resources*, such as natural-Gas-fired Power Plants (GPPs), i.e., the technical ability of flexibility resources to deviate from their operating point in a controlled way. This balancing must be accomplished on multiple time scales, ranging from seconds

(inertia response) to years (variation of seasonal energy generation and demand). In addition, spatial scales in terms of grid voltage levels and geographic locations of flexibility resources must be considered when aggregating (small-scale) flexibility resources (Sarstedt et al. 2021; Gazafroudi et al. 2018) and to account for transmission constraints (Bucher et al. 2015a). Flexibility, flexibility requirements as well as flexibility potentials are typically measured in terms of *power, ramp-rate* and *duration (energy)* (Ulbig and Andersson 2015). For example, a GPP without a lower operational power limit and with a maximum power of 100 MW, a ramp-rate of 10 MW/min and a scheduled operating point of 80 MW has a *positive* flexibility potential of 20 MW available after 2 min for a given duration and a *negative* flexibility potential of 80 MW available after 8 min.

Flexibility potentials are usually provided by centrally coordinated flexibility resources like GPPs or Pumped Hydroelectric Energy Storages (PHES). However, the energy transition leads to a shift in generation from centralized to decentralized, small-scale generation units, and thus also to a shift in flexibility resources (Riaz and Mancarella 2021; Kalantar-Neyestanaki and Cherkaoui 2021). Therefore, other types of flexibility resources need to be explored to (at least partially) replace GPPs, for example, especially as they are based on natural gas, which is also a scarce resource today. Furthermore, according to BDEW (2022), the gross electricity generation from renewable energy in Germany, for example, more than doubled from 123.8 TWh to 256.2 TWh between 2011 and 2022, and will continue to grow. This also leads to greater variability and uncertainty associated with renewable generation, resulting in an increasing need for additional flexibility resources.

An emerging technology that can serve as a flexibility resource in the future are Battery Storage Systems (BSS). For example, according to the "Market Master Data Register" (MaStR) (Bundesnetzagentur für Elektrizität, Gas, Telekommunikation, Post und Eisenbahnen 2023) around half a million BSSs with a total capacity of 4.39 GWh are already in operation in Germany. However, most of them are currently not controllable by an energy system operator and, thus, cannot be used directly as a flexibility resource. *Nevertheless, the question arises whether the flexibility potential of currently installed BSSs in general could already replace the flexibility potential of some, and how many, GPPs*. The focus on GPPs is particularly interesting because they use a scarce fossil fuel while also being used as flexibility resource, as commonly mentioned in literature (e.g., Lannoye et al. 2012; Lund et al. 2015; Heinen et al. 2017). The objective of this work is to answer *the question* and motivate the use of already installed BSSs as flexibility resources. For this purpose, openly available data from the MaStR and open_eGo (Hülk et al. 2017) are used to spatially aggregate the multi-time-scale flexibility potential of BSSs and compare it to the flexibility potential of GPPs. To the best of our knowledge, we are the first to combine geospatial data with analysis of multi-time-scale flexibility potentials, while previous work had focused mainly on spatial mapping of energy generation and consumption data (e.g., Hülk et al. 2017; Singh et al. 2015). The specific contributions of this paper are as follows:

- Selection and adaptation of a flexibility model from literature to quantify the multi-time-scale flexibility potential of flexibility resources. In addition, we combine the flexibility model with two methods for spatially aggregating the flexibility potentials.

- Analysis of the openly available MaStR data in terms of completeness, consistency and suitability, and definition of evaluation setups (e.g., considering all BSSs or only remotely controllable BSSs) based on the available parameters.
- Evaluation of the potential of existing (aggregated) BSSs for a possible replacement of GPPs based on the defined setups and using the adapted flexibility model.

Note, in this work the focus is on BSSs, i.e., stationary storages, because they have characteristics similar to GPPs. In particular, both flexibility resources are in general fully controllable and have a fixed location. To further reduce dependence on GPPs, Electric Vehicles (EVs) would be an interesting additional option, but they are more difficult to control for pragmatic reasons. For example, EVs are not stationary and not available 24/7, making them more challenging to replace the services offered by GPPs. Furthermore, Wallboxes are not yet widely deployed, and charging may be limited to a few hours (e.g., 3 h per day per EV), such as at corporate charging stations. In addition, car rental companies have many EVs, but they may be charged at different locations depending on the car tenant.

The remainder of the paper is organized as follows: Existing approaches for modeling flexibility potentials are described in the "Related work" section. Modeling and aggregation of multi-time-scale flexibility potentials of BSSs and GPPs are introduced in the "Methodology" section. The "Data analysis" section presents the analysis of the MaStR data. The results of applying the methodology to the MaStR data are presented in the "Results" section. Finally, the "Conclusion" section summarizes the work and suggests directions for future research.

Related work

Existing models for quantifying the flexibility potential of flexibility resources can be broadly classified into *quality metrics* (e.g., Ma et al. 2013; Zhao et al. 2016), *machine learning models* (e.g., MacDougall et al. 2016; Förderer et al. 2018), and *envelopes* (e.g. Bucher et al. 2015b; Ulbig and Andersson 2015; Riaz and Mancarella 2021; Nosair and Bouffard 2015; Šikšnys et al. 2015). In Ma et al. (2013), for example, a quality metric for the flexibility potential of flexibility resources, in this case conventional generators, is introduced based on technical constraints (ramp-rate, power) of these flexibility resources. This quality metric is used to determine optimal investments in flexibility resources for a power system. In Zhao et al. (2016), a quality metric is proposed in the form of an indicator function whose output value 1 corresponds to the availability of sufficient flexibility potential in a power system within a certain time interval, otherwise it has output value 0. This quality metric can be used as a situational awareness tool for power system operators. The Artificial Neural Networks (ANNs) proposed in MacDougall et al. (2016); Förderer et al. (2018) intend to predict how long a power deviation from a operating set point can be sustained (MacDougall et al. 2016), check the feasibility of load profiles, create price-based load profile forecasts, generate load profiles, and validate and repair load profiles (Förderer et al. 2018). These ANNs can be used, for example, as part of an energy management system.

Besides quality metrics and machine learning models, most of the flexibility models analyzed are classified as envelopes. In Ulbig and Andersson (2015), for example, a polytope

is used that covers possible operating set point deviations of a flexibility resource in terms of power, ramp rate, and energy for a given time interval. A similar model is proposed in Bucher et al. (2015b), but several consecutive time intervals are considered. In addition, Riaz and Mancarella (2021) introduces P-Q charts approximated as polytopes to describe possible operating set point deviations of a flexibility resource in terms of active (P) and reactive (Q) power for a given time interval. The envelopes considered so far correspond to mathematical sets, in particular polytopes. In contrast, the flexibility model proposed in Nosair and Bouffard (2015) is based on two time series representing a lower and an upper bound on possible active power deviations of a flexibility resource under given constraints such as ramp-rate and energy limitations. Another flexibility model worth mentioning is presented in Šikšnys et al. (2015). This model quantifies flexibility potentials in terms of a time interval in which an energy flexibility potential can be requested and an energy profile that provides a time series of upper and lower bounds on energy flexibility potentials.

With the exception of the quality metric in Ma et al. (2013), all flexibility models briefly outlined require time series data to quantify flexibility potentials. The required time series data correspond to the scheduled operation of flexibility resources (e.g., active power set points or State of Charge (SoC) over time). The scope of these flexibility models (Bucher et al. 2015b; Ulbig and Andersson 2015; Riaz and Mancarella 2021; Zhao et al. 2016; MacDougall et al. 2016; Förderer et al. 2018; Nosair and Bouffard 2015; Šikšnys et al. 2015) is primarily the optimal operation of a power system, and the flexibility models are used to consider the balancing of flexibility requirements with flexibility potentials.

For answering the *question* from the "Introduction" section, none of the flexibility models reviewed seem suitable for several reasons:

1. For large-scale power systems, as in the case of Germany, there are no time series data reflecting the operation of each installed BSS (about half a million in Germany) and each GPP.
2. The flexibility models operate on a single time scale (e.g., 15 min time intervals), which is determined by the time resolution of the time series data used. Therefore, to evaluate flexibility potentials on multiple time scales (e.g., 1 s or 5 min time intervals), time series data with different time resolutions are needed. However, such data are also not available for each BSS and GPP (e.g., in Germany).
3. Without (substantial) changes, the flexibility models do not allow aggregation and comparison of the flexibility potentials of different flexibility resources, taking into account the geographic location of flexibility resources.

Therefore, in this paper, a flexibility model recently published by Li et al. (2022) is adapted to address these issues. The details of this flexibility model and the proposed adaptations are discussed in the "Methodology" section.

Methodology

The methodology consists of two parts. First, the "Flexibility potential modeling" subsection introduces the modeling of the multi-time-scale flexibility potential of both BSS and GPP. Second, the "Flexibility potential aggregation" subsection describes the temporal and spatial aggregation of the modeled flexibility potential, which is required to compare

the flexibility potential of BSSs to that of GPPs. The terms multi-time-scale flexibility potential and flexibility potential are used interchangeably in the remainder of this work.

Flexibility potential modeling

To quantify the flexibility potential of a flexibility resource r as defined in Definition 1, the model of Li et al. (2022) is adopted and adapted, with the adaptations as described in the following.

Definition 1 A flexibility resource r is mathematically defined by its rated energy $\overline{E}_r \in \mathbb{R}_{>0}$ [in kWh], rated power $\overline{P}_r \in \mathbb{R}_{>0}$ [in kW], ramp-up rate $\overline{R}_r^{pos} \in \mathbb{R}_{>0}$ [in kW/h], ramp-down rate $\overline{R}_r^{neg} \in \mathbb{R}_{>0}$ [in kW/h] and geographic location $\big((latitude, longitude) \in \mathbb{R}^2\big)$, i.e., $r = \big(\overline{E}_r, \overline{P}_r, \overline{R}_r^{pos}, \overline{R}_r^{neg}, (latitude, longitude)\big)$.

The modeling assumption underlying the flexibility model (Li et al. 2022) is that a flexibility potential is considered as a flexibility potential under ideal conditions. For example, to quantify the positive flexibility potential of a BSS, a SoC of 100% and a scheduled discharge power of 0 kW are assumed. Accordingly, a SoC of 0% and a scheduled charge power of 0 kW are assumed for the negative flexibility potential. Based on this modeling assumption, the flexibility model aims at quantifying multi-time-scale flexibility potentials by mapping the rated energy $\overline{E}_r$ and power $\overline{P}_r$ of a flexibility resource r to a characteristic domain, which is referred to as the time interval domain in this paper. The mapping results in upper bounds on the *positive energy flexibility potential* $FP_r^{pos}(\tau)$ and *negative energy flexibility potential* $FP_r^{neg}(\tau)$ of flexibility resource r for any time interval, i.e., any time scale, $\tau \in \mathbb{R}_{>0}$ [in hours]. Let $\overline{P}_{r,t}^{pos}, \overline{P}_{r,t}^{neg} \in [0, \overline{P}_r]$ denote the maximum available power generation (positive flexibility potential) and maximum available power consumption (negative flexibility potential), respectively, of a flexibility resource r at a given time $t \in [0, \tau]$. In contrast to Li et al. (2022), both FP_r^{pos} and FP_r^{neg} are modeled as functions that are monotonically increasing in τ:

$$FP_r^{pos}(\tau) = min(\int_0^\tau \overline{P}_{r,t}^{pos}\, dt, \overline{E}_r), \tag{1}$$

$$FP_r^{neg}(\tau) = min(\int_0^\tau \overline{P}_{r,t}^{neg}\, dt, \overline{E}_r). \tag{2}$$

For example, a BSS with $\overline{E}_r = 30$ kWh, $\overline{P}_r = 30$ kW and $\overline{P}_{r,t}^{pos} = \overline{P}_r\, \forall t \in [0, \tau]$ can provide a maximum positive flexibility potential of 15 kWh for $\tau = 0.5$ h according to Equation (1), and 30 kWh for $\tau = 1$ h. A visual example for FP_r^{pos} is presented in Fig. 1 of the "Results" section. In Li et al. (2022), FP_r^{neg} is modeled as a function monotonically decreasing in τ, i.e., $FP_r^{neg'}(\tau) = \overline{E}_r - \int_0^\tau \overline{P}_{r,t}^{neg}\, dt$. Negative flexibility potentials, however, refer to generation curtailment, and GPPs can generally be curtailed for indefinite periods. Hence, in the worst case $\overline{E}_r = \infty$, which can be handled by Equation (2), but not with the alternative $FP_r^{neg'}$ from Li et al. (2022).

In addition to power and energy, ramp-rate is a third measure used to quantify flexibility potentials (cf. "Introduction" section). Although not explicitly considered in Li et al. (2022),

ramp-up rate $\overline{R}_r^{pos}$ and ramp-down rate $\overline{R}_r^{neg}$ can be included in Equations (1) and (2) by setting:

$$\overline{P}_{r,t}^{pos} = min\left(t \cdot \overline{R}_r^{pos}, \overline{P}_r\right), \tag{3}$$

$$\overline{P}_{r,t}^{neg} = min\left(t \cdot \overline{R}_r^{neg}, \overline{P}_r\right). \tag{4}$$

Note, in Equations (3) and (4) it is assumed that power ramps linearly and that a flexibility resource initially has zero power output and input because $\overline{P}_{r,0}^{pos} = 0$ kW and $\overline{P}_{r,0}^{neg} = 0$ kW. These assumptions can be relaxed by setting $\overline{P}_{r,t}^{pos} = \overline{P}_r$ and $\overline{P}_{r,t}^{neg} = \overline{P}_r \; \forall t \in [0, \tau]$, which results again in an upper bound on the flexibility potential when applied to Equations (1) and (2).

The presented model does not require time series data like operating set points of flexibility resources, thus rated power and other flexibility resource master data as provided by the MaStR are sufficient to quantify flexibility potentials. This type of flexibility potential, which represents the flexibility potential under ideal conditions, is also referred to as *theoretical* flexibility potential in Zhang et al. (2021). In contrast, most other models in literature (cf. "Related work" section) focus on *actual* or *achievable* flexibility potentials on a single time scale, i.e., those models take additional constraints (e.g., response time of a GPP) and current operating conditions (e.g., SoC of a BSS) of flexibility resources into account. However, planning the operation of flexibility resources is not the scope in this paper (cf. "Introduction" section), thus focusing on the quantification of the theoretical flexibility potentials seems adequate.

Flexibility potential aggregation

Aggregation of the modeled flexibility potentials is performed in both the temporal and spatial dimensions. For the temporal or time interval aggregation, respectively, the approach presented in Li et al. (2022) is adapted, which is briefly described in the "Temporal aggregation" subsection. In the "Spatial aggregation" subsection, spatial aggregation based on Voronoi cells (Boots et al. 2009) is introduced and combined with the multi-time-scale flexibility potential model.

Temporal aggregation

In Li et al. (2022), aggregation of the multi-time-scale flexibility potential is performed by approximating the aggregate flexibility potential of a set R of flexibility resources (cf. Definition 1) using piecewise-linear functions. The slopes and endpoints of the linear functions are derived from the rated energy $\overline{E}_r$ and power $\overline{P}_r$ of flexibility resources $r \in R$. That approach is elegant because it does not initially require computations of FP_r^{pos} and FP_r^{neg} for each flexibility resource. However, it does not allow for a direct integration of ramp-rate characteristics. For this reason and because multi-time-scale flexibility potentials being additive in the time interval domain (Li et al. 2022), the aggregation is performed using Equations (5) and (6):

$$FP_R^{pos}(\tau) = \sum_{r \in R} FP_r^{pos}(\tau), \tag{5}$$

$$FP_R^{neg}(\tau) = \sum_{r \in R} FP_r^{neg}(\tau). \tag{6}$$

Spatial aggregation

For spatial aggregation, two different approaches are proposed. The first method, **M1**, clusters and aggregates BSSs by taking GPPs as center points of Voronoi cells. Thus, **M1** allows for comparing the flexibility potential of a GPP with the aggregated flexibility potential of BSSs located in the vicinity of this GPP. With Definition 1, the geographic location of a flexibility resource corresponds to a point in the Euclidean plane $\mathbb{R}^2$. Let $C \subset \mathbb{R}^2$ denote the set of geographic locations of GPPs, i.e., the center points, and let d_E denote the Euclidean distance metric. Then, for each $gpp \in C$ the Voronoi cell V_{gpp} is defined as:

$$V_{gpp} = \{x \in \mathbb{R}^2 \mid d_E(x, gpp) \leq d_E(x, c), \forall c \in C \setminus \{gpp\}\}. \tag{7}$$

Based on the obtained Voronoi cells, the flexibility potentials of BSSs are aggregated for each Voronoi cell using Equations (5) and (6), with set R consisting of the BSSs located in V_{gpp}. While **M1** compares the flexibility potentials of BSSs and GPPs by taking into account regionality, the method has the drawback of being oblivious to grid transmission constraints (cf. "Results" section). For example, a BSS located close to a GPP may nevertheless be connected to a completely different part of the grid due to parallel power lines.

In contrast, the second method, **M2**, takes into account the topology of the power grid by using the medium-voltage (MV) grid districts from Hülk et al. (2017). These grid districts represent a combination of Voronoi cells with substations as center points and municipal boundaries, thus leading to a more realistic power grid clustering than using vanilla Voronoi cells. For each grid district, the flexibility potentials of the contained BSSs are again aggregated using Equations (5) and (6). However, unlike **M1**, most Voronoi cells will not contain a GPP, as the number of municipalities in Germany, for example, exceeds the number of GPPs installed by far. Thus, **M2** is particularly useful to draw conclusions about the extent to which BSSs can contribute flexibility potentials compared to a *reference* GPP, assumed to be installed in each grid district (cf. "Results" section).

Data analysis

The MaStR is a comprehensive state register containing master data of German power/gas generation and consumption units as well as market players (Bundesnetzagentur für Elektrizität, Gas, Telekommunikation, Post und Eisenbahnen 2023). In principle, all stationary power generation units that are directly or indirectly connected to the power grid are subject to registration, regardless of size and time of commissioning. The deadline for registration of new units is one month from the date of commissioning of the unit, so the MaStR is fairly complete. At the time of this data analysis, there are 599,814 registered storage units, which include BSSs (415,290 units) and other technologies (e.g., PHES), and 83,641 registered gas-based power generation units, which include GPPs (378 units) and other technologies (e.g., Stirling engine). Although the master data are

entered by the unit operators, the data for each unit are verified by the grid operator. To ensure consistency in the data used, only units with completed verification are included in this work.

In addition to filtering for completed verification, answering the *question* from the "Introduction" section requires the application of additional filter criteria, based on the available MaStR parameters. For the storage units, only those with *battery* technology are considered which are geographically located on the German mainland and are not permanently taken off the grid. For gas-based power generation units, the following filter criteria apply: Energy carrier is *natural gas*, technology is *gas turbine*, remotely controllable (by grid operator, marketer, or third party), and in operation. Although there are other gas-based technologies such as Stirling engines, the focus here is on gas turbines because they are often referred to in literature as flexibility resources (Lund et al. 2015; Heinen et al. 2017). A filter based on the minimum bid size as required for balancing power (e.g., 5 MW for 15 min in Germany) is not applied as the focus in this work is on available flexibility potentials in general. Statistical data on the units or flexibility resources after applying the relevant filters are shown in Table 1. Note that the total number of BSSs (415,290) exceeds that of GPPs (378) by far. However, only 9795 BSSs are currently remotely controllable by the grid operator. Moreover, the average net rated power of BSSs is merely a fraction of that of a GPP. Nevertheless, these statistics are a first indicator that, once remotely controllable, BSSs can substitute at least some GPPs by aggregating their flexibility potential.

From the "Methodology" section is known that for quantifying flexibility potentials at least data on geographic location, power and energy limits, and possibly ramp-rates are required. For power, two parameters exist in the MaStR: *gross power* and *net rated power*. For GPPs, the net rated power is used to exclude the power plants' own consumption (e.g., for auxiliary equipment), which is part of the gross power and cannot be provided as flexibility potential. For the BSSs, the net rated power is also used, which is the minimum of gross power (i.e., maximum power in continuous operation) and associated converter power. As for energy, the usable storage capacity is given for the BSSs, while this information cannot be provided for GPPs. However, the flexibility model introduced allows the definition of an infinite energy limit (cf. "Flexibility potential modeling" subsection), which for GPPs still corresponds to an upper bound on the flexibility potential and is therefore a reasonable choice. Besides, ramp-rates

Table 1 Statistics about GPPs and BSSs from the MaStR, used in the "Results" section

Parameter	GPP	BSS
Total number of units	378	415,290
Total net rated power	9.97 GW	2.68 GW
Average net rated power	26,371.30 kW	6.45 kW
Total energy capacity	N/A	4.39 GWh
Average energy capacity	N/A	10.56 kWh
Remote control	378	9795
Technology	Gas turbine with waste heat boiler Gas turbine without waste heat boiler Gas turbine with downstream steam turbine	Battery

are not included in the MaStR, but can in principle be derived from the technology used. For example, a comparison of six gas turbines in Abudu et al. (2021) shows ramp-rates between 6 and 15% of rated power per minute, so an assumed ramp-rate of 10%/min would be reasonable for gas turbines. Ramp-rates of BSSs are negligible compared to those of GPPs because the fast converters of BSSs are capable of delivering nearly instantaneous power changes (in range of milliseconds) (Dozein and Mancarella 2019; Danner et al. 2021). BSS ramp-rates are therefore neglected in this work. For the spatial allocation of the flexibility resources, the MaStR provides geographic coordinates and/or the municipality. Especially for private BSSs, the coordinates are usually confidential. In this case, geocoding is used for estimating the location (latitude, longitude) based on the address information. Furthermore, a GPP may have multiple gas turbines, so the net rated power of the gas turbines that have the same geographic coordinates are summed.

In summary, the MaStR data are sufficient for the parameterization of the multi-time-scale flexibility potential model. With respect to the considered flexibility resources, the following two basic evaluation setups are defined:

S1 All GPPs (without ramp-rate) and all BSSs from Table 1.
S2 All GPPs (without ramp-rate) and remotely controllable BSSs from Table 1.

In addition, two setups are defined that consider a ramp-rate of 10%/min for the GPPs:

S3 All GPPs (ramp-rate 10%/min) and all BSSs from Table 1.
S4 All GPPs (ramp-rate 10%/min) and remotely controllable BSSs from Table 1.

Results

This section presents the results for the evaluation setups **S1**–**S4** and spatial flexibility aggregation methods **M1** and **M2**. Note, only results for the positive flexibility potential are given, since the focus is on the *theoretical* flexibility potential (cf. "Flexibility potential modeling" subsection), which is symmetric. Before going into detail, Fig. 1 shows the aggregated positive flexibility potential of all GPPs with and without ramping constraint and all as well as only remotely controllable BSSs in Germany (cf. Equation 5). Considering the more realistic setup, i.e., GPPs with ramp-rates, all BSSs could replace all GPPs for time scales up to about 300 s (i.e., 5 min) when the BSSs are fully charged. Considering only the remotely controllable BSSs or relaxing the ramping constraint of the GPPs, this is not feasible.

To account not only for temporal aspects but also for regional variations, Fig. 2 shows the results of applying **M1** to the setup **S1** for time scales $\tau = 0.25$ h (i.e., 15 min), 1 h, and 4 h. The ratio for each Voronoi cell is calculated by Equation (8), with $R = \{bss \mid (latitude, longitude)\ of\ bss \in V_{gpp}\}$:

$$Ratio(\tau, gpp) = \frac{FP_R^{pos}(\tau)}{FP_{gpp}^{pos}(\tau)}. \tag{8}$$

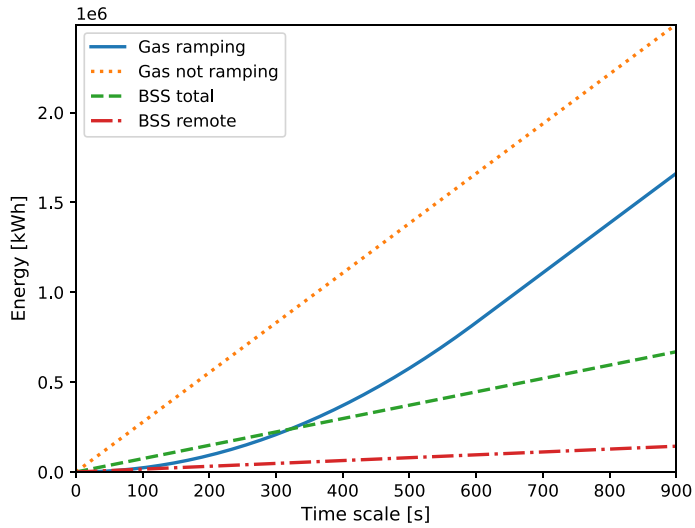

Fig. 1 Aggregated positive flexibility potential of GPPs and BSSs selected from the MaStR (cf. Table 1) assuming an SoC of 100%

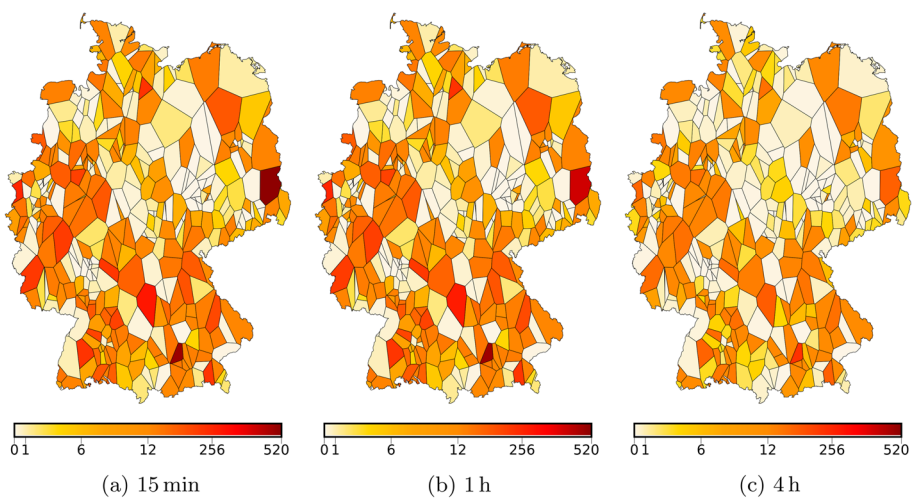

Fig. 2 Ratio of aggregated positive flexibility potential of BSSs (initial SoC 100%) to positive flexibility potential of the corresponding GPP in Germany (cf. Equation (8)) for time scales 15 min, 1 h and 4 h (**M1**, **S1**)

Ratios greater than 1 therefore imply that the BSSs are able to fully replace the corresponding GPP in terms of theoretical flexibility potential on the given time scale. The first finding from these maps is that there is generally less BSS flexibility potential to replace GPPs in Eastern Germany. Nevertheless, the ability of existing BSSs to replace GPPs is fairly well distributed across Germany. The largest number of high ratios is observed in Southern and Western Germany, which also correlates with the large number of installed BSSs (281,616) in this area. Furthermore, high ratios are observed particularly for the smaller time scales (15 min, 1 h), but even for the large time scale of 4 h more than 50% of the Voronoi cells still have ratios beyond 1. In

addition, there are cells with extremely high ratios, especially in Fig. 2a. Here, the high ratio (greater 500) of the cell in Southern Germany can be explained by a total of 3341 BSSs in this cell (the average per cell are 1125 BSSs). Another outlier cell (again, ratio greater than 500) is located in Eastern Germany with 1560 BSSs and one extremely large BSS with a net rated power of 66 MW. Similar explanations can be found for the other outliers. Consequently, the BSSs in cells with high ratios could share their flexibility potential with other (neighboring) cells to replace the flexibility potential of even more GPPs.

The results of applying **M1** to the setup **S2** are given in Fig. 3. It is observed that the remotely controlled BSSs are again well distributed over Germany. However, taking into account regionality and BSSs that can be controlled remotely, the theoretical flexibility potential of only a few GPPs can be replaced (many ratios below 1). A notable exception is the cell in Eastern Germany, where, among others, the large BSS (66 MW) is remotely controllable. The maps based on the application of **M1** to setups **S3** and **S4** are intentionally omitted as they provide limited additional value. In contrast to Figs. 2 and 3, the maps for **S3** and **S4** show higher ratios due to the ramp-rate of 10%/min used, which is indirectly proportional to the ratio, but the spatial distribution across Germany remains the same.

While Fig. 2 shows that in many cells fully charged BSSs could replace the installed GPP on time scales up to several hours, another interesting aspect is how long the aggregated flexibility potential of BSSs would theoretically last per cell compared to the GPP. In terms of the methodology used, this corresponds to the time scale at the intersection of the aggregated flexibility potential of the BSSs in a cell and the flexibility potential of the corresponding GPP. In Fig. 1 and considering all BSSs and all GPPs (with ramping) in Germany, for example, this time scale is about 300 s. The result of this analysis performed per cell is shown in Fig. 4. In the figure, the time scales at which the individual GPPs in Germany start to have greater flexibility potentials than the BSSs in their respective Voronoi cells are summarized in box plots. The box plots

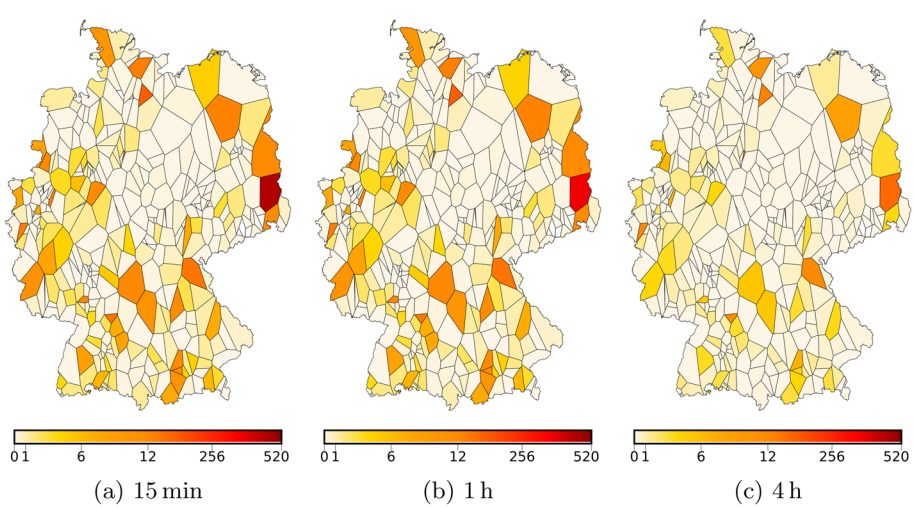

Fig. 3 Ratio of aggregated positive flexibility potential of BSSs (initial SoC 100%) to positive flexibility potential of the corresponding GPP in Germany (cf. Equation 8) for time scales 15 min, 1 h and 4 h (**M1**, **S2**)

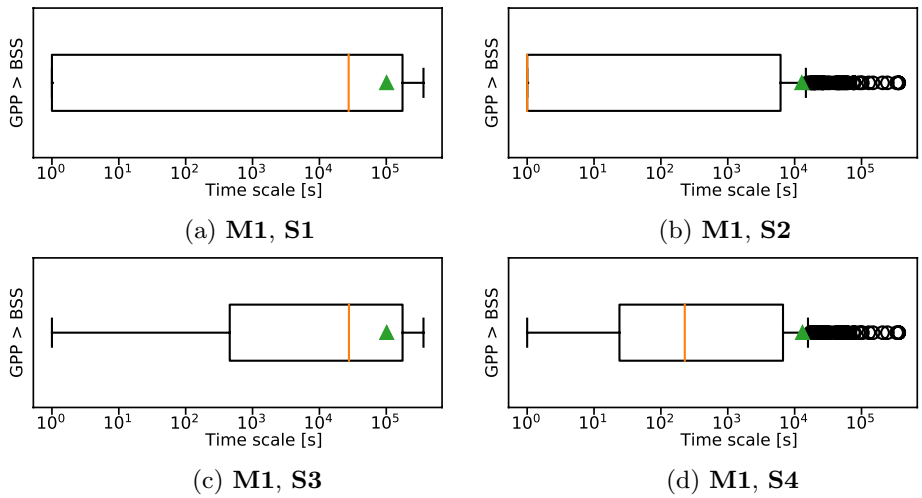

Fig. 4 Time scales at which the individual GPPs start to have greater positive flexibility potentials than the aggregated BSSs for setups **S1**–**S4** and aggregation method **M1**. The mean time scale is represented as a triangle

reveal that for setup **S1**, on average (cf. triangle symbol), the flexibility potential of the GPP exceeds that of the BSSs on time scales greater than 10^5 s or 28 h, respectively (median about $2.7 \cdot 10^4$ s or 8 h). In more than 25%, however, this time scale is 1 s, which means that the GPP can always provide a greater flexibility potential than the BSSs. On the other hand, considering setup **S3** and thus ramp-rates for the GPPs (cf. Figure 4c), the first quartile corresponds to 456 s or 7.6 min, respectively. The other statistical characteristics such as the mean time scale are similar for both setup **S1** (without GPP ramp-rates) and setup **S3** (with GPP ramp-rates) as the GPPs ramp-up fast at 10%/min. Of course, for setups **S2** and **S4** the same behavior is observed with respect to the ramp-rates. In addition, Fig. 4b and d confirm that by using only the flexibility potential of remotely controllable BSSs, the flexibility potential of the GPPs can often be replaced on time scales up to a few minutes, if at all.

In Fig. 5 the ratios (Equation 8) computed for all Voronoi cells are summarized as box plots for all defined evaluation setups. For the 15-min and 1-h time scales, similar mean ratios are observed in each of Fig. 5a and b, while the mean ratios for the 4-h time scale are significantly lower. In Fig. 5a, for example, the mean ratio for the 1-h time scale is 26.46 and for the 4-h time scale is 11.51, i.e., the ratios more than halved on average. This can be explained by the fact that many BSSs have similar or identical power and energy limits and therefore the flexibility potentials cannot increase further after 1 h. For example, a BSS with a power limit of 50 kW and an energy limit of 50 kWh can only provide a maximum positive flexibility potential of 50 kWh for all time scales greater than 1 h, assuming the BSS is not recharged in between. Looking at the ramping behavior of the GPPs (**S3**), the box plots for 1 h and 4 h are similar to those for **S1**. Thus, as expected for a (high) ramp-rate of 10%/min, differences between **S1** and **S3** are primarily visible for smaller time scales such as 15 min. For instance, the ratios almost double on average when comparing the 15-min time scale for **S1** and **S3**. Besides, it can be observed in Fig. 5b and d that by exclusively using

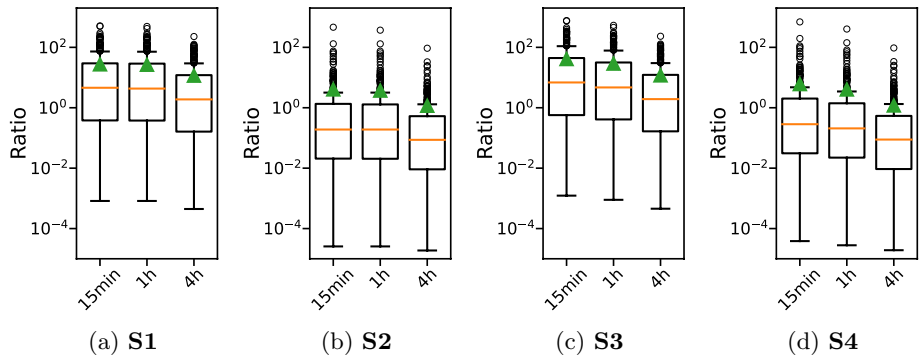

Fig. 5 Ratio of aggregated positive flexibility potential of BSSs (initial SoC 100%) to positive flexibility potential of the corresponding GPP in Germany (cf. Equation 8) for time scales 15 min, 1 h and 4 h (**M1**). The mean ratio is represented as a triangle

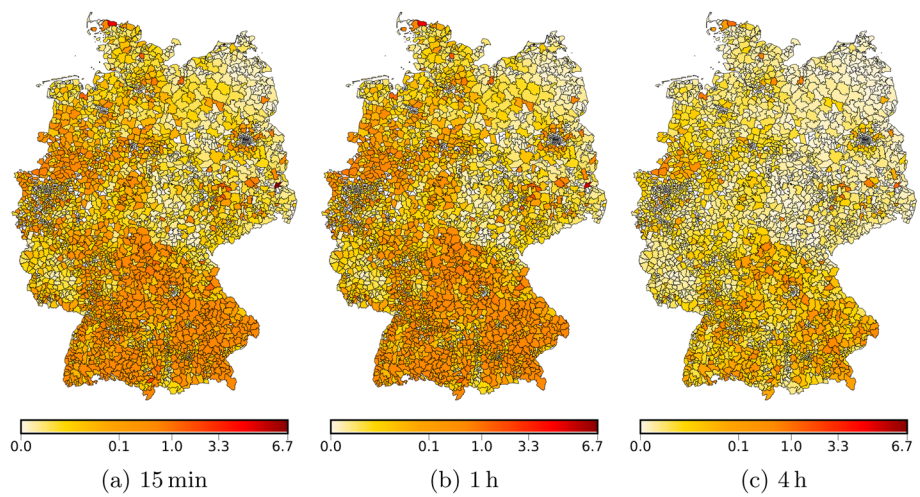

Fig. 6 Ratio (cf. Equation 8) of aggregated positive flexibility potential of BSSs (initial SoC 100%) in Germany to positive flexibility potential of a reference GPP (net rated power: 10 MW) for time scales 15 min, 1 h and 4 h (**M2**, **S1**)

remotely controllable BSSs and regardless of the consideration of ramp-rates, about 75% (third quartile) of the GPPs could not be replaced (i.e., ratios below 1). However, to return to the *question* in the "Introduction" section: *If all BSSs were remotely controllable and regionality was taken into account, the theoretical flexibility potential of more than 65% of GPPs (with and without ramp-rates) in Germany can be replaced on time scales up to 1 h (cf. Figure* 5a *and* c) *and often even on larger time scales (e.g., 55% of the GPPs in Germany on the 4-h time scale)*. A first step to replace the flexibility potential of GPPs is therefore to equip BSSs with remote control and to develop suitable business models that take into account both the objectives of grid operators (e.g., optimizing flexibility) and the objectives of BSS owners (e.g., optimizing self-consumption).

The spatial flexibility aggregation method **M2** is applied to the evaluation setups defined in the "Data analysis" section using a reference GPP with net rated power 10 MW. This leads to the following findings. Figure 6 confirms the results regarding the potential of BSSs in Southern and Western Germany to replace GPPs in terms of

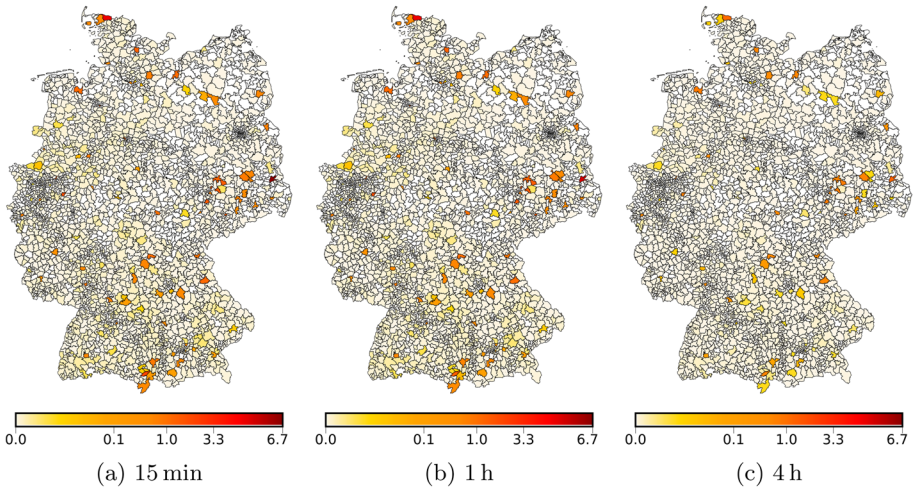

Fig. 7 Ratio (cf. Equation 8) of aggregated positive flexibility potential of BSSs (initial SoC 100%) in Germany to positive flexibility potential of a reference GPP (net rated power: 10 MW) for time scales 15 min, 1 h and 4 h (**M2**, **S2**)

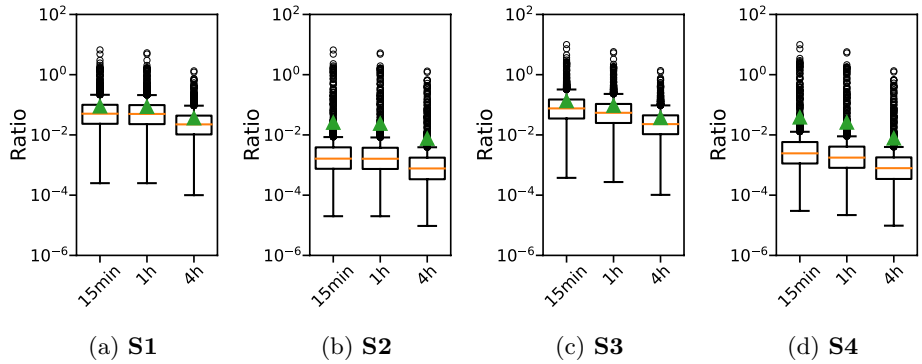

Fig. 8 Ratio (cf. Equation 8) of aggregated positive flexibility potential of BSSs (initial SoC 100%) in Germany to positive flexibility potential of the reference GPP (net rated power: 10 MW) for time scales 15 min, 1 h and 4 h (**M2**). The mean ratio is represented as a triangle

flexibility (cf. Figure 2). Nevertheless, it is very unlikely that the BSSs of a single Voronoi cell can replace the flexibility potential of the reference GPP (mean ratio below 1, see Fig. 8a). However, the maps show, especially on time scales of 15 min and 1 h, that the BSSs of several neighboring cells can achieve the replacement of a single reference GPP. In contrast to **M1**, this substitution is even more realistic because neighboring cells correspond to different municipalities and therefore likely have separate MV grids (concession agreements in Germany), i.e., transmission constraints are more relaxed. In contrast, when only remotely controllable BSSs are considered, the cells with higher ratios are more isolated (cf. Figure 7), and 1333 of 3606 cells do not even have a remotely controllable BSS. Besides, it can be seen in Fig. 8 that regardless of the setup, more than 75% of the cells do not have enough flexibility potential of BSSs to substitute the reference GPP (ratios below 1), with two notable outliers in Eastern and Northern Germany due to BSSs with net rated powers above 45 MW (cf.

Figure 6). Note, in Fig. 8 cells without BSSs are omitted for reasons of visibility, so the mean ratios and quartiles would actually be even lower.

Regardless of the spatial flexibility aggregation method used, the methodology and results presented are optimistic due to the modeling assumption of flexibility potentials under ideal conditions (cf. "Flexibility potential modeling" subsection). Contrasting the strengths and limitations of this optimistic approach, the methodology allows, on the one hand, the derivation of valid upper bounds on the positive and negative flexibility potential that a flexibility resource can provide at any time scale. And, compared to other existing flexibility models (cf. "Related work" section), deriving these upper bounds does not require time series data related to the scheduled operation of flexibility resources. On the other hand, not taking into account the scheduled operation of flexibility resources is also the main limitation of the methodology and the results, as it leads to rather optimistic upper bounds for the flexibility potential. For example, in a private household with a PV power plant and a BSS used to optimize self-consumption and autarchy, the BSS is typically charged during the day and discharged at night (e.g., Danner et al. 2021). This means that the SoC of the BSS is almost never 100% or 0%. The same applies to the scheduled charge/discharge power, which is almost never 0 kW in this example. To overcome this limitation and obtain more realistic results for the Germany example, data on the operation of each BSS or at least its target behavior (e.g., self-consumption optimization) and data on the operation of each GPP would be required. However, as mentioned in the "Related work" section, there is no data source that provides such information for each BSS and GPP in Germany. Alternatively, it is conceivable to use an estimate of the scheduled operation of BSSs and GPPs. For example, market data from (Bundesnetzagentur fur Elektrizitat, Gas, Telekommunikation, Post und Eisenbahnen) could be used, which provides aggregated GPP and PV energy generation data for Germany over time. The total GPP energy generation could be disaggregated to the GPPs in Germany, e.g., by considering their rated power. Assuming that the existing BSSs are charged with PV power plants, the total PV energy generation could be (partially) disaggregated to these BSSs, possibly taking into account demand, weather and PV/BSS location data. Note that, in principle, the methodology already supports consideration of the scheduled operation of flexibility resources. In particular, $\overline{P}_{r,t}^{pos}$ and $\overline{P}_{r,t}^{neg}$ would need to be set appropriately, and in the case of a BSS, $\overline{E}_r$ would need to be based on its actual or estimated SoC (cf. Equations 1 and 2).

Conclusion

In this paper, we analyze the potential of BSSs to possibly replace GPPs in terms of flexibility potential, using Germany as an example. The methodology is based on a generic multi-time-scale flexibility potential model, parameterized with openly available data from the MaStR and open_eGo. It provides a first indication that especially in Southern and Western Germany, and in general, about 65% of the theoretical flexibility potential of GPPs could be replaced by existing BSSs at the respective sites. This should also be an incentive to make currently non-remotely controllable BSSs remotely controllable, thereby reducing dependence on fossil fuels to provide flexibility.

The potential analysis is theoretical in nature and addresses flexibility resources without their actual operation and transmission constraints (apart from the approximation

by the flexibility potential aggregation method **M2**). An extension with market data to derive actually used flexibility potentials, i.e., the integration of dynamic data with master data from MaStR, could be valuable, for example. In addition, openly available power grid infrastructure data (e.g., from OpenStreetMap) can be used to better reflect transmission constraints. Finally, the energy that a BSS can provide in the form of positive flexibility potential must first be supplied by another energy source (e.g., a nearby PV power plant), so (renewable) generation capacity and how it would need to be expanded to appropriately charge BSSs is another open topic (*theoretical* versus *achievable* flexibility potentials).

Author contributions

ML initiated the research topic, conceptualized the methodology and evaluation, and is the main writer. LS implemented the methodology and performed the data analysis and evaluation. HdM provided research direction, supervision, and helped to write the final version of the paper. All authors read and approved the final manuscript.

About this supplement

This article has been published as part of Energy Informatics Volume 6 Supplement 1, 2023: Proceedings of the 12th DACH+ Conference on Energy Informatics 2023. The full contents of the supplement are available online at https://energyinformatics.springeropen.com/articles/supplements/volume-6-supplement-1.

Funding

This work was funded by the Deutsche Forschungsgemeinschaft (DFG, German Research Foundation)—project "Formal modeling of operational flexibility in multi-scale multi-modal energy systems" (project number 450860949)—as part of the priority program DFG SPP 1984: Hybrid and multimodal energy systems: System theoretical methods for the transformation and operation of complex networks.

Availability of data and materials

The datasets used in this work (MaStR, open_eGo) are publicly available. The implementation of the flexibility model and the evaluation are available on request from the corresponding author.

Declarations

Competing interests

The authors declare that they have no competing interests.

Published: 19 October 2023

References

Abudu K, Igie U, Minervino O, Hamilton R (2021) Gas turbine efficiency and ramp rate improvement through compressed air injection. Proc Inst Mech Eng Part A: J Power Energy 235(4):866–884

BDEW (2022) Gross electricity generation from renewable energy in Germany from 1990 to 2022 (in terawatt hours) [Graph]. https://www.statista.com/statistics/583179/gross-electricity-generation-from-renewable-energy-germany/

Boots B, Sugihara K, Chiu SN, Okabe A (2009) Spatial tessellations: concepts and applications of voronoi diagrams

Bucher MA, Chatzivasileiadis S, Andersson G (2015a) Managing flexibility in multi-area power systems. IEEE Trans Power Syst 31(2):1218–1226

Bucher MA, Delikaraoglou S, Heussen K, Pinson P, Andersson G (2015b) On quantification of flexibility in power systems. In: 2015 IEEE Eindhoven PowerTech, pp. 1–6

Bundesnetzagentur für Elektrizität, Gas, Telekommunikation, Post und Eisenbahnen: Marktstammdatenregister. https://www.marktstammdatenregister.de/MaStR/. Data as of February 08, 2023

Bundesnetzagentur für Elektrizität, Gas, Telekommunikation, Post und Eisenbahnen: SMARD - Strommarktdaten für Deutschland. https://www.smard.de/home

Danner D, Seidemann J, Lechl M, de Meer H (2021) Flexibility disaggregation under forecast conditions. In: Proceedings of the Twelfth ACM International Conference on Future Energy Systems, pp. 27–38

Dozein MG, Mancarella P (2019) Application of utility-connected battery energy storage system for integrated dynamic services. In: 2019 IEEE Milan PowerTech, pp. 1–6. IEEE

Gazafroudi AS, Prieto-Castrillo F, Pinto T, Corchado JM (2018) Energy flexibility management in power distribution systems: decentralized approach. In: 2018 International Conference on Smart Energy Systems and Technologies (SEST), pp. 1–6. IEEE

Förderer K, Ahrens M, Bao K, Mauser I, Schmeck H (2018) Modeling flexibility using artificial neural networks. Energy Inf 1(1):73–91

Heinen S, Hewicker C, Jenkins N, McCalley J, O'Malley M, Pasini S, Simoncini S (2017) Unleashing the flexibility of gas: innovating gas systems to meet the electricity system's flexibility requirements. IEEE Power Energy Magazine 15(1):16–24
Hülk L, Wienholt L, Cußmann I, Müller UP, Matke C, Kötter E (2017) Allocation of annual electricity consumption and power generation capacities across multiple voltage levels in a high spatial resolution. Int J Sustain Energy Plan Manag 13:79–92
Huo Y, Bouffard F, Joós G (2020) Spatio-temporal flexibility management in low-carbon power systems. IEEE Trans Sustain Energy 11(4):2593–2605
Kalantar-Neyestanaki M, Cherkaoui R (2021) Coordinating distributed energy resources and utility-scale battery energy storage system for power flexibility provision under uncertainty. IEEE Trans Sustain Energy 12(4):1853–1863
Lannoye E, Flynn D, O'Malley M (2012) Evaluation of power system flexibility. IEEE Trans Power Syst 27(2):922–931
Li H, Zhang N, Bao W, Fan Y, Dong L, Cai P (2022) Modeling and planning of multi-timescale flexible resources in power systems. CSEE J Power Energy Syst
Lund PD, Lindgren J, Mikkola J, Salpakari J (2015) Review of energy system flexibility measures to enable high levels of variable renewable electricity. Renew Sustain Energy Rev 45:785–807
Ma J, Silva V, Belhomme R, Kirschen DS, Ochoa LF (2013) Evaluating and planning flexibility in sustainable power systems. In: 2013 IEEE Power & Energy Society General Meeting, pp. 1–11
MacDougall P, Kosek AM, Bindner H, Deconinck G (2016) Applying machine learning techniques for forecasting flexibility of virtual power plants. In: 2016 IEEE Electrical Power and Energy Conference (EPEC), pp. 1–6
Nosair H, Bouffard F (2015) Flexibility envelopes for power system operational planning. IEEE Trans Sustain Energy 6(3):800–809
Riaz S, Mancarella P (2021) Modelling and characterisation of flexibility from distributed energy resources. IEEE Trans Power Syst 37(1):38–50
Sarstedt M, Kluß L, Gerster J, Meldau T, Hofmann L (2021) Survey and comparison of optimization-based aggregation methods for the determination of the flexibility potentials at vertical system interconnections. Energies 14(3):687
Šikšnys L, Valsomatzis E, Hose K, Pedersen TB (2015) Aggregating and disaggregating flexibility objects. IEEE Trans Knowl Data Eng 27(11):2893–2906
Singh A, Eser P, Chokani N, Abhari R (2015) High resolution modeling of the impacts of exogenous factors on power systems-case study of Germany. Energies 8(12):14168–14181
Ulbig A, Andersson G (2015) Analyzing operational flexibility of electric power systems. Int J Electrical Power Energy Syst 72:155–164
Zhang P, Lu X, Li K (2021) Achievable energy flexibility forecasting of buildings equipped with integrated energy management system. IEEE Access 9:122589–122599
Zhao J, Zheng T, Litvinov E (2016) A unified framework for defining and measuring flexibility in power system. IEEE Trans Power Syst 31(1):339–347

Publisher's Note